

Supporting Information

Regulating the Magnetic Dynamics of Mononuclear β -Diketone Dy(III) Single-Molecule Magnets through Substitution Effect on Capping N-Donor Coligands

Jing Xi,^{a#} Xiufang Ma,^{a,d#} Peipei Cen,^b Yuwei Wu,^a Yi-Quan Zhang,^{*,c} Yan Guo,^a Jinhui Yang,^{*,a} Danian Tian,^b and Xiangyu Liu^{*,a,d}

^a State Key Laboratory of High-efficiency Utilization of Coal and Green Chemical Engineering, College of Chemistry and Chemical Engineering, Ningxia University, Yinchuan 750021, China

^b College of Public Health and Management, Ningxia Medical University, Yinchuan 750021, China

^c Jiangsu Key Laboratory for NSLSCS, School of Physical Science and Technology, Nanjing Normal University, Nanjing 210023, China

^d State Key Laboratory of Coordination Chemistry, Nanjing University, Nanjing, 210023, China

These authors contributed equally to this work.

*Corresponding author

Dr. Xiangyu Liu

E-mail: xiangyuliu432@126.com

Prof. Jinhui Yang

E-mail: lyjhmp@163.com

Prof. Yi-Quan Zhang

zhangyiquan@njnu.edu.cn

Contents

1. *Ab initio* calculational details.

2. References

Fig. S1 View of the complexes **1-5** molecular structure with thermal ellipsoids drawn at 50% probability level

Fig. S2 Crystal packing diagram for complex **1**

Fig. S3 Crystal packing diagram for complex **2**

Fig. S4 Crystal packing diagram for complex **3**

Fig. S5 Crystal packing diagram for complex **4**

Fig. S6 Crystal packing diagram for complex **5**

Fig. S7 PXRD curves of **1** (a), **2** (b), **3** (c), **4** (d) and **5** (e)

Fig. S8 Plots of $\chi_M T$ vs $\log T$ for **1** (a), **2** (b), **3** (c), **4** (d) and **5** (e).

Fig. S9 M vs. H/T data for complexes **1-5** at different temperatures.

Fig. S10 M vs. H curves for **1** (a), **2** (b), **3** (c), **4** (d) and **5** (e) at 2 K. The red lines correspond to the *PHI* calculations.

Fig. S11 Temperature dependent in-phase (χ') of the ac susceptibilities for **1** (a), **2** (b), **3** (c), **4** (d) and **5** (e) under zero dc field.

Fig. S12 Frequency dependent in-phase (χ') of the ac susceptibilities for **1** (a), **2** (b), **3** (c), **4** (d) and **5** (e) under zero dc field.

Fig. S13 Temperature dependent in-phase (χ') of the ac susceptibilities for **1** (a), **2** (b), **3** (c), **4** (d) and **5** (e) under the external dc fields.

Fig. S14 Frequency dependent in-phase (χ') of the ac susceptibilities for **1** (a), **2** (b), **3** (c), **4** (d) and **5** (e) under the external dc fields.

Fig. S15 Cole-Cole plots under the static dc fields for **1** (a), **2** (b), **3** (c), **4** (d) and **5** (e). The solid lines represent the best fit to the measured results.

Table S1. Crystal Data and Structure Refinement Details for **1-5**

Table S2. Selected bond lengths (Å) and bond angles (°) for **1-5**

Table S3. Dy (III) ions geometry analysis of **1-5** by SHAPE 2.1 software.

Table S4. Relevant structural parameters in square anti-prism geometry, α angle and ϕ angle for **1-4**

Table S5. Crystal field parameters for **1-5** fitted from $\chi_M T$ vs. T and M vs. H simultaneously

Table S6. Energy levels and g for **1-5** fitted from $\chi_M T$ vs. T and M vs. H simultaneously

Table S7. Relaxation fitting parameters from least-squares fitting of $\chi(f)$ data under zero dc field of **1**

Table S8. Relaxation fitting parameters from least-squares fitting of $\chi(f)$ data under zero dc field of **2**

Table S9. Relaxation fitting parameters from least-squares fitting of $\chi(f)$ data under zero dc field of **3**

Table S10. Relaxation fitting parameters from least-squares fitting of $\chi(f)$ data under zero dc field of **4**

Table S11. Relaxation fitting parameters from least-squares fitting of $\chi(f)$ data under zero dc field of **5**

Table S12. Relaxation fitting parameters from least-squares fitting of $\chi(f)$ data under 1500 Oe dc field of **1**.

Table S13. Relaxation fitting parameters from least-squares fitting of $\chi(f)$ data under 1200 Oe dc field of **2**.

Table S14. Relaxation fitting parameters from least-squares fitting of $\chi(f)$ data under 1200 Oe dc field of **3**.

Table S15. Relaxation fitting parameters from least-squares fitting of $\chi(f)$ data under 1200 Oe dc field of **4**.

Table S16. Relaxation fitting parameters from least-squares fitting of $\chi(f)$ data under 1200 Oe dc field of **5**.

Table S17. Calculated energy levels (cm⁻¹), g (g_x , g_y , g_z) tensors and predominant m_J values of the lowest eight Kramers doublets (KDs) of complexes **1-5** using CASSCF/RASSI-SO with MOLCAS 8.4.

Table S18. Wave functions with definite projection of the total moment $| m_J \rangle$ for the lowest two KDs of complexes **1-5** using CASSCF/RASSI-SO with MOLCAS 8.4.

1. *Ab initio* calculational details

Complete-active-space self-consistent field (CASSCF) calculations on complexes **1–5** on the basis of single-crystal X-ray determined geometry have been carried out with MOLCAS 8.4^{S1} program package.

The basis sets for all atoms are atomic natural orbitals from the MOLCAS ANO-RCC library: ANO-RCC-VTZP for Dy^{III}; VTZ for close O and N; VDZ for distant atoms. The calculations employed the second order Douglas-Kroll-Hess Hamiltonian, where scalar relativistic contractions were taken into account in the basis set and the spin-orbit couplings were handled separately in the restricted active space state interaction (RASSI-SO) procedure. For complexes **1–5**, active electrons in 7 active spaces include all *f* electrons (CAS(9 in 7)) in the CASSCF calculation. To exclude all the doubts, we calculated all the roots in the active space. We have mixed the maximum number of spin-free state which was possible with our hardware (all from 21 sextets, 128 from 224 quadruplets, 130 from 490 doublets). SINGLE_ANISO^{S2} program was used to obtain the energy levels, *g* tensors, predominant *m_J* values, magnetic axes, *et al.*, based on the above CASSCF/RASSI-SO calculations.

2. References

- 1) F. Aquilante, J. Autschbach, R. K. Carlson, L. F. Chibotaru, M. G. Delcey, L. De Vico, I. Fdez. Galván, N. Ferré, L. M. Frutos, L. Gagliardi, M. Garavelli, A. Giussani, C. E. Hoyer, G. Li Manni, H. Lischka, D. Ma, P. Å. Malmqvist, T. Müller, A. Nenov, M. Olivucci, T. B. Pedersen, D. Peng, F. Plasser, B. Pritchard, M. Reiher, I. Rivalta, I. Schapiro, J. Segarra-Martí, M. Stenrup, D. G. Truhlar, L. Ungur, A. Valentini, S. Vancoillie, V. Veryazov, V. P. Vysotskiy, O. Weingart, F. Zapata, R. Lindh, MOLCAS 8: New Capabilities for Multiconfigurational Quantum Chemical Calculations across the Periodic Table, *J. Comput. Chem.*, 2016, **37**, 506.
- 2) (a) Chibotaru, L. F.; Ungur, L.; Soncini, A. *Angew. Chem. Int. Ed.*, **2008**, *47*, 4126. (b) Ungur, L.; Van den Heuvel, W.; Chibotaru, L. F. *New J. Chem.*, 2009, **33**, 1224. (c) Chibotaru, L. F.; Ungur, L.; Aronica, C.; Elmoll, H.; Pilet, G.; Luneau, D. *J. Am. Chem. Soc.*, 2008, **130**, 12445.

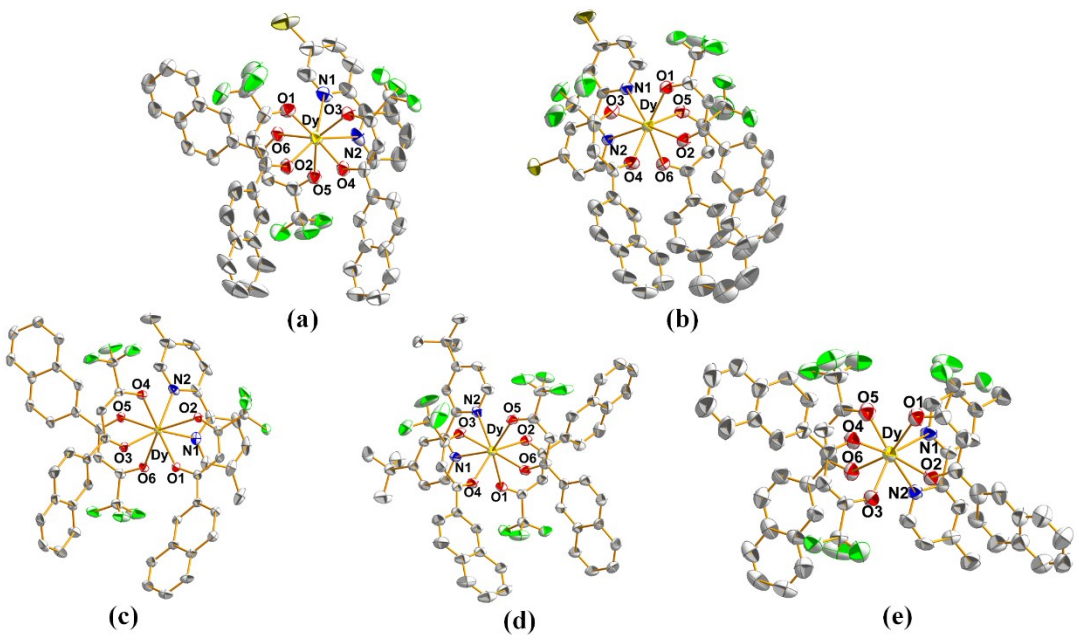


Fig. S1 View of the complexes **1-5** molecular structure with thermal ellipsoids drawn at 50% probability level (Dy yellow, Br gold, O red, N blue, F green, C grey). H atoms are omitted for clarity.

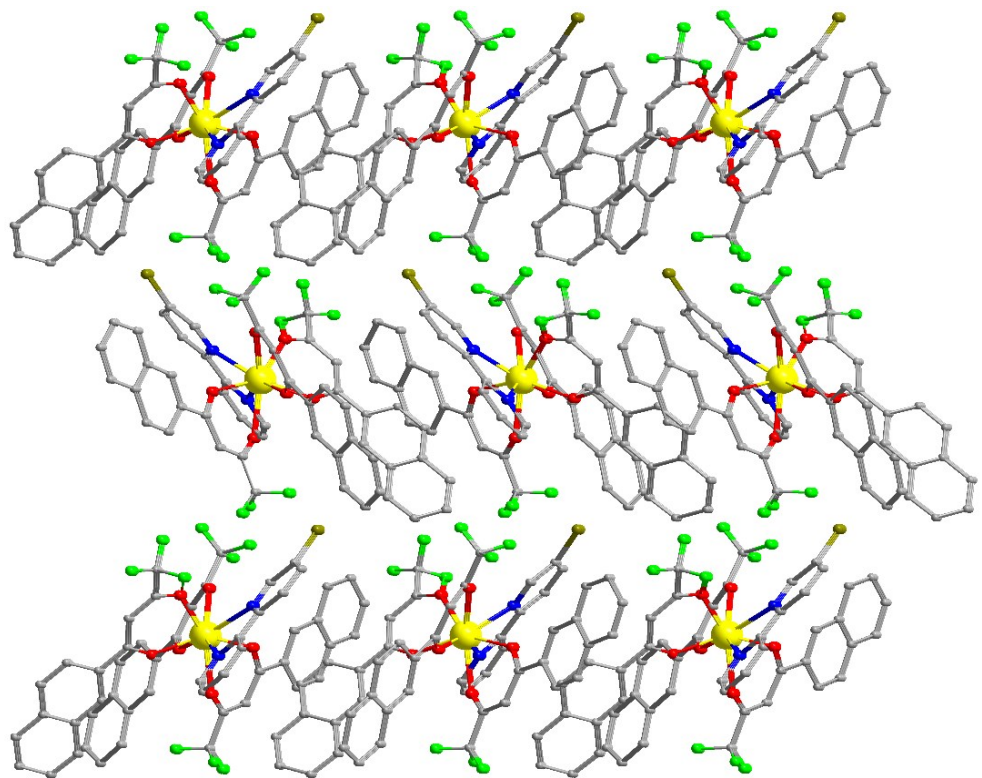


Fig. S2 Crystal packing diagram for complex **1**

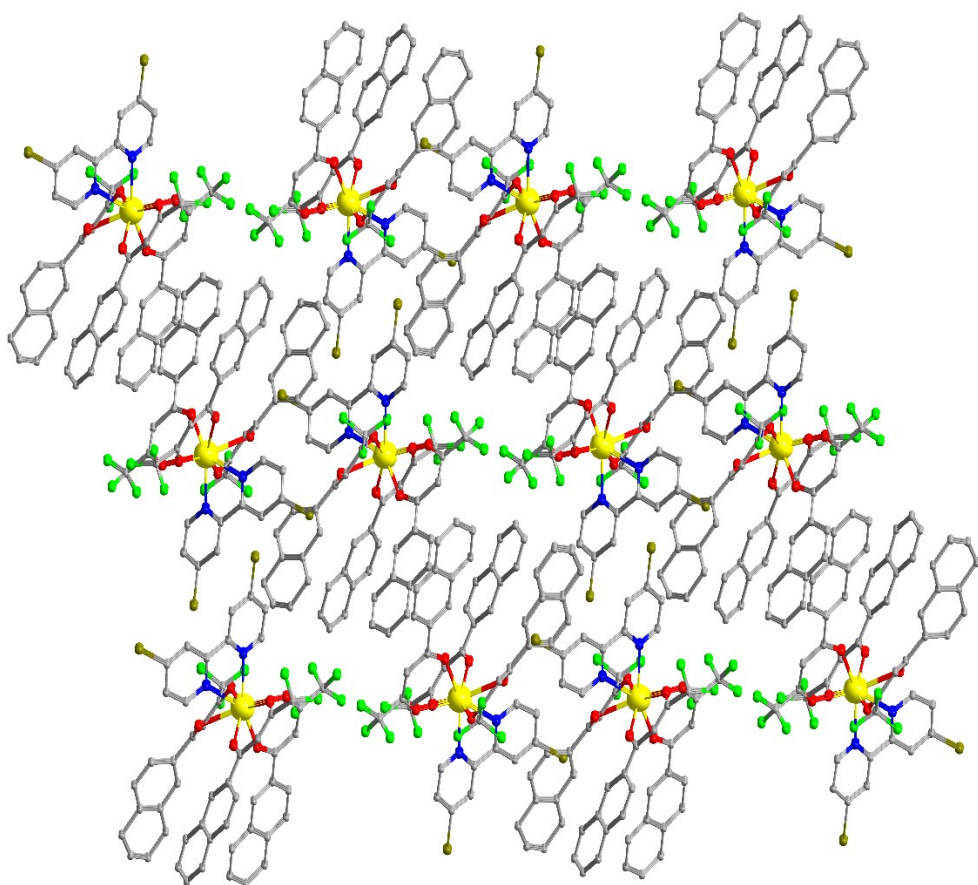


Fig. S3 Crystal packing diagram for complex 2

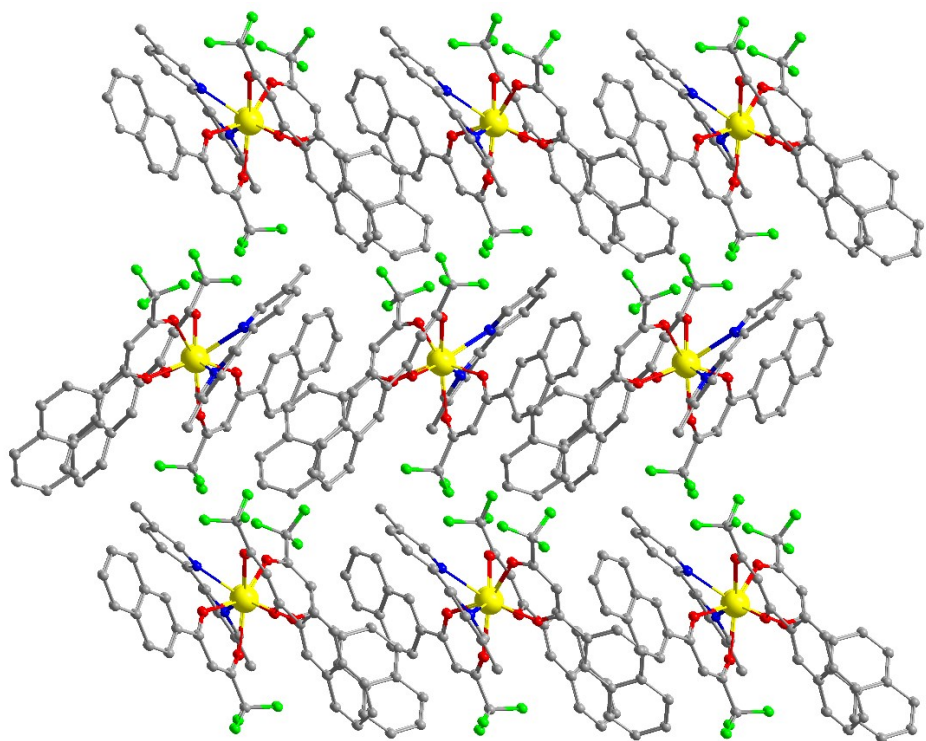


Fig. S4 Crystal packing diagram for complex 3

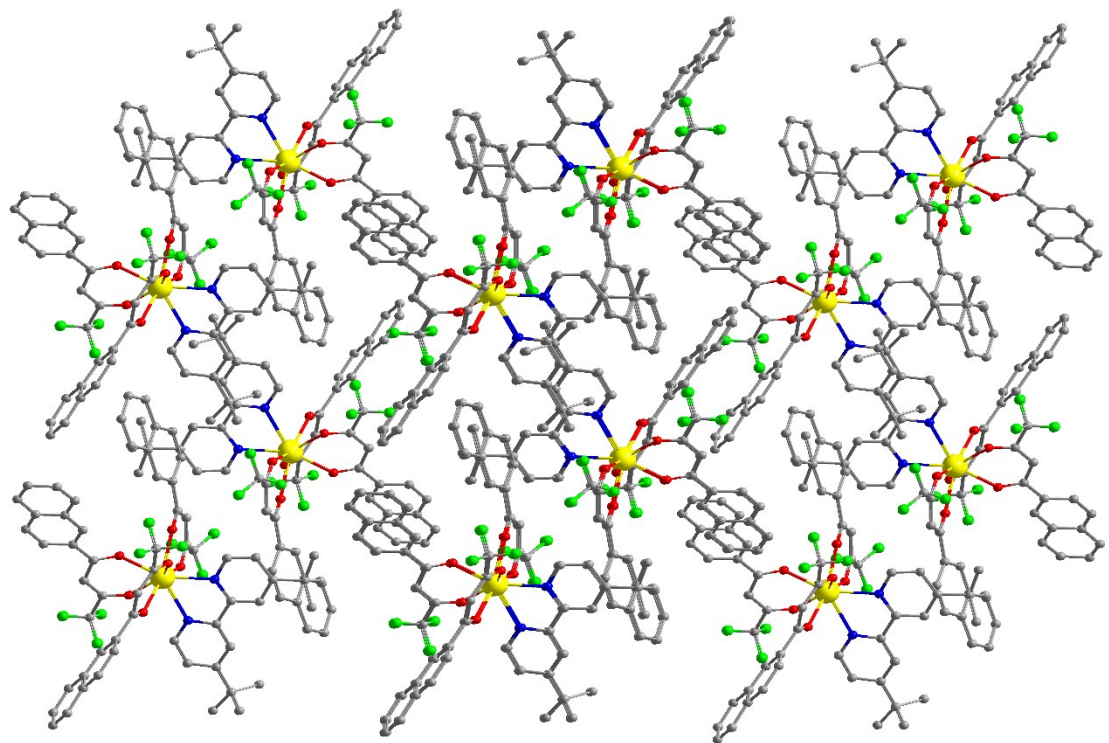


Fig. S5 Crystal packing diagram for complex 4

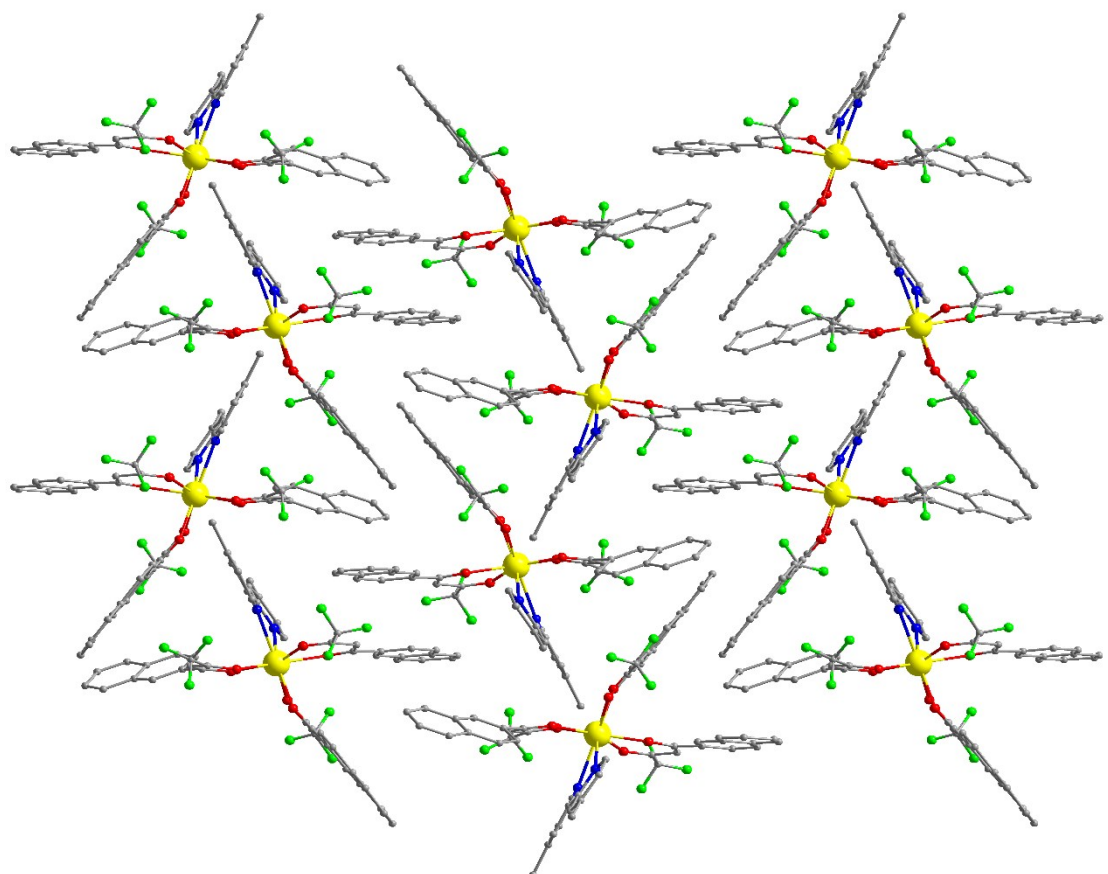


Fig. S6 Crystal packing diagram for complex 5

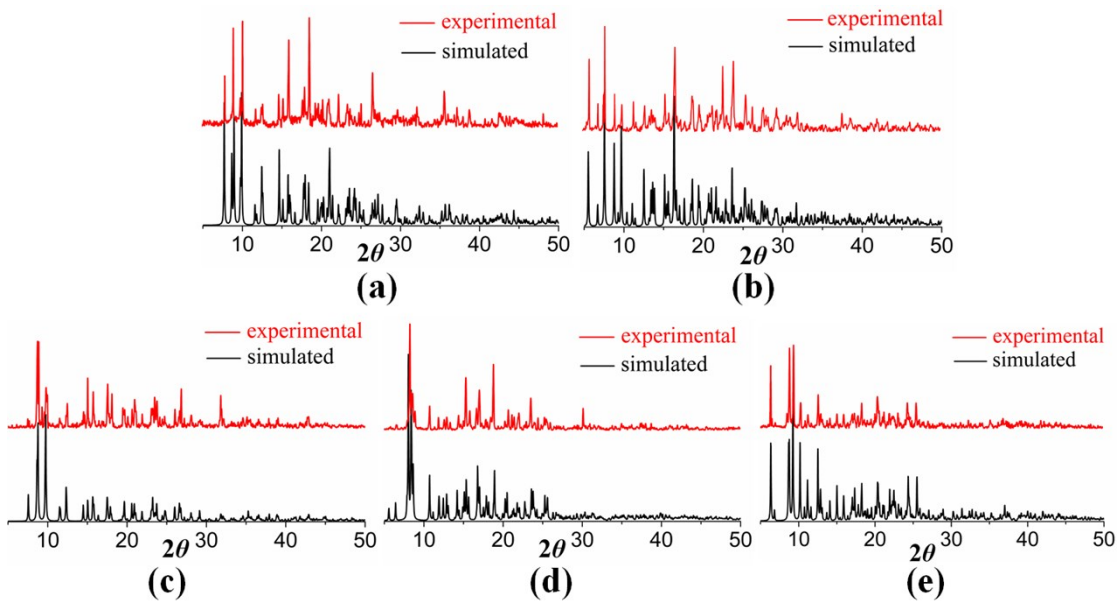


Fig. S7 PXRD curves of **1** (a), **2** (b), **3** (c), **4** (d) and **5** (e).

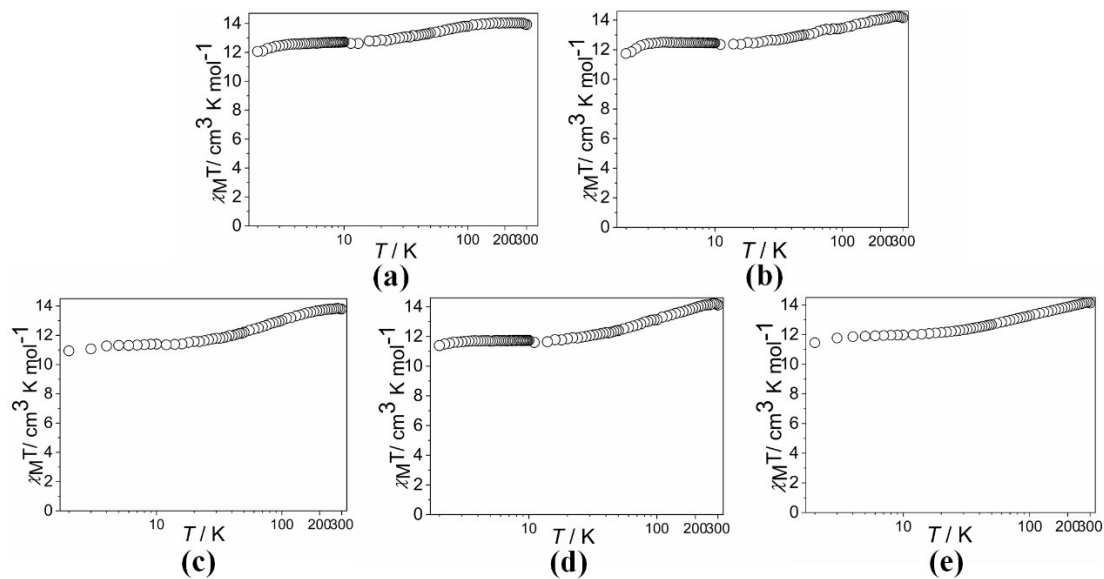


Fig. S8 Plots of $\chi_M T$ vs $\log T$ for **1** (a), **2** (b), **3** (c), **4** (d) and **5** (e).

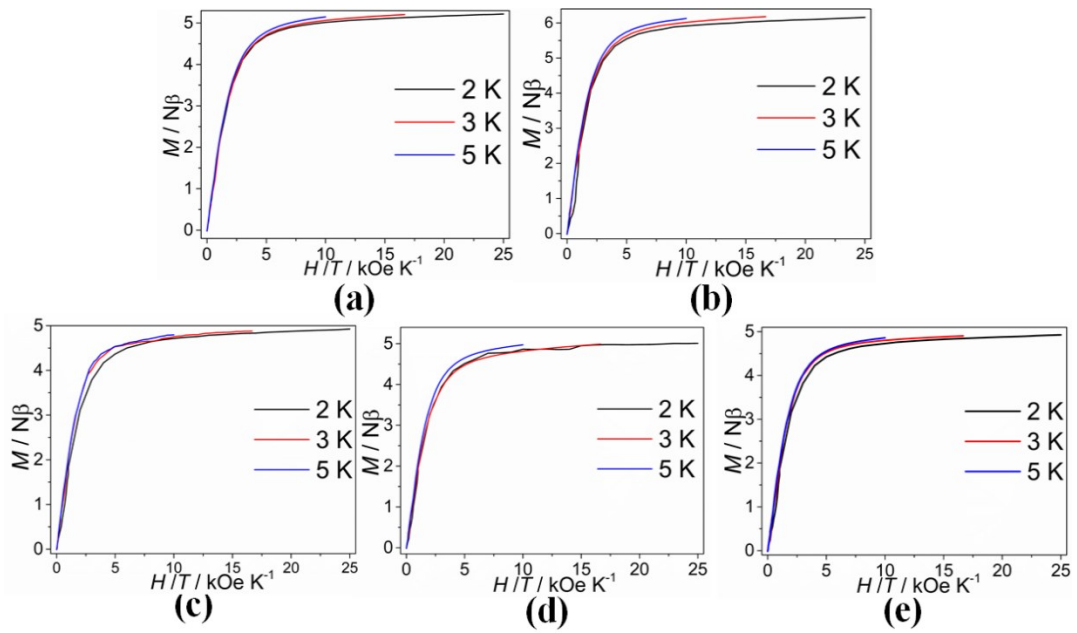


Fig. S9 M vs. H/T data for complexes **1-5** at different temperatures.

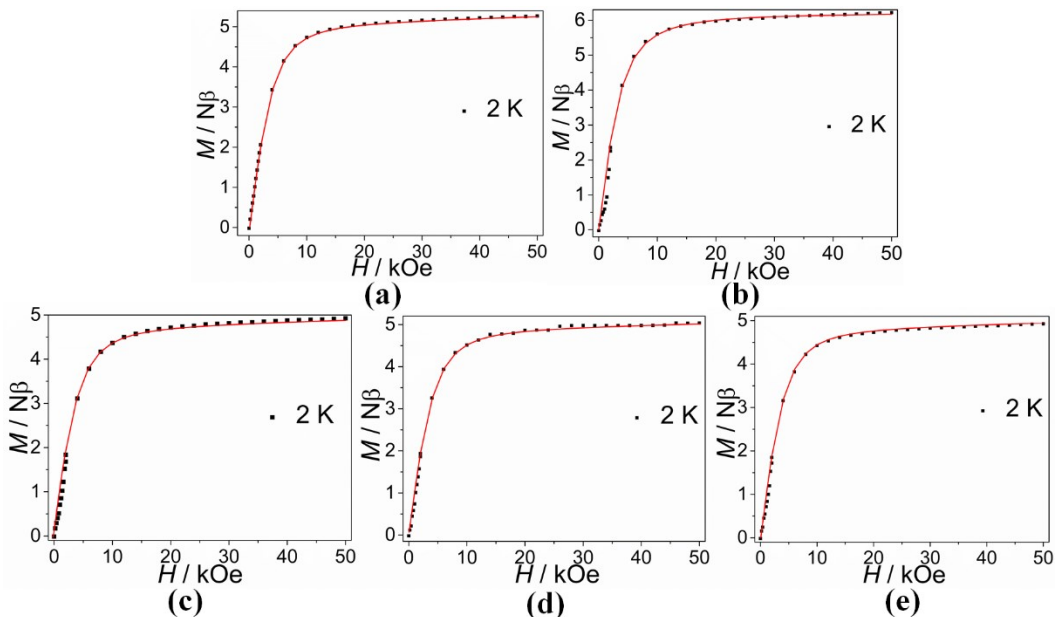


Fig. S10 M vs. H curves for **1** (a), **2** (b), **3** (c), **4** (d) and **5** (e) at 2 K. The red lines correspond to the *PHI* calculations.

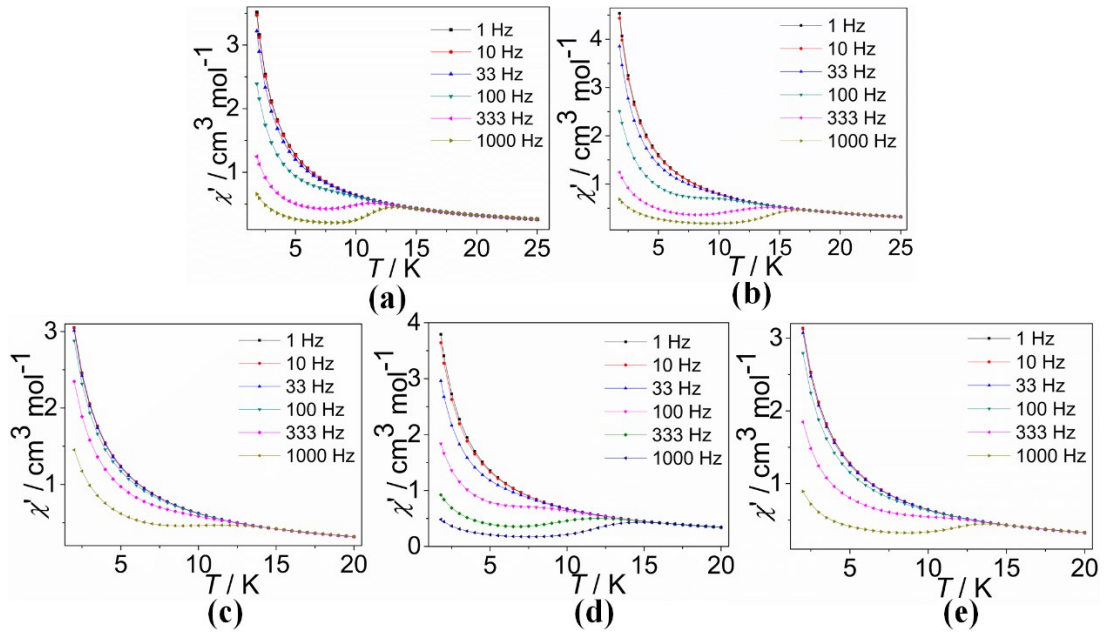


Fig. S11 Temperature dependent in-phase (χ') of the ac susceptibilities for **1** (a), **2** (b), **3** (c), **4** (d) and **5** (e) under zero dc field.

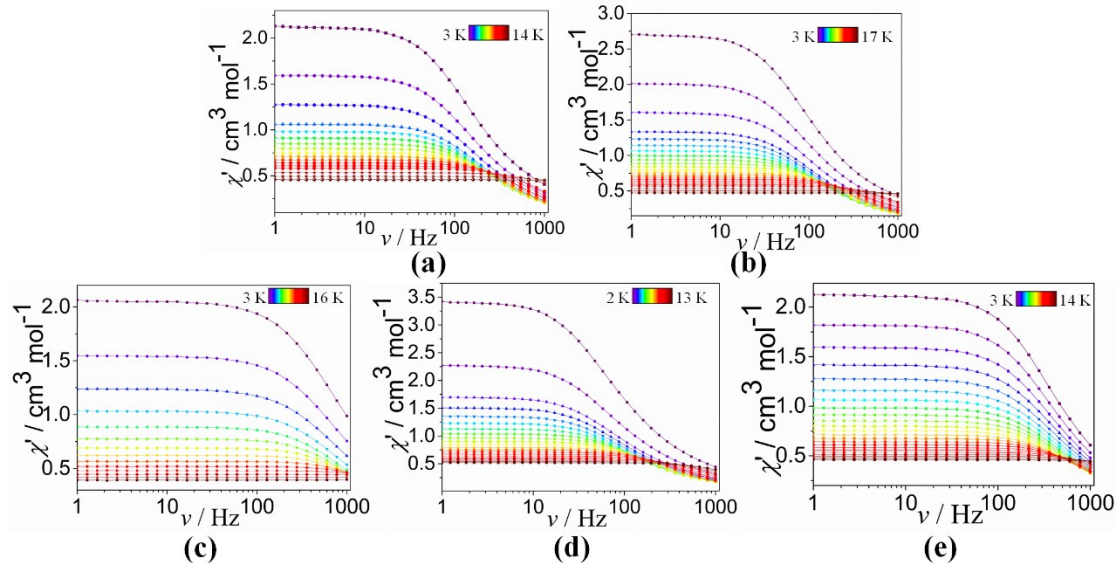


Fig. S12 Frequency dependent in-phase (χ') of the ac susceptibilities for **1** (a), **2** (b), **3** (c), **4** (d) and **5** (e) under zero dc field.

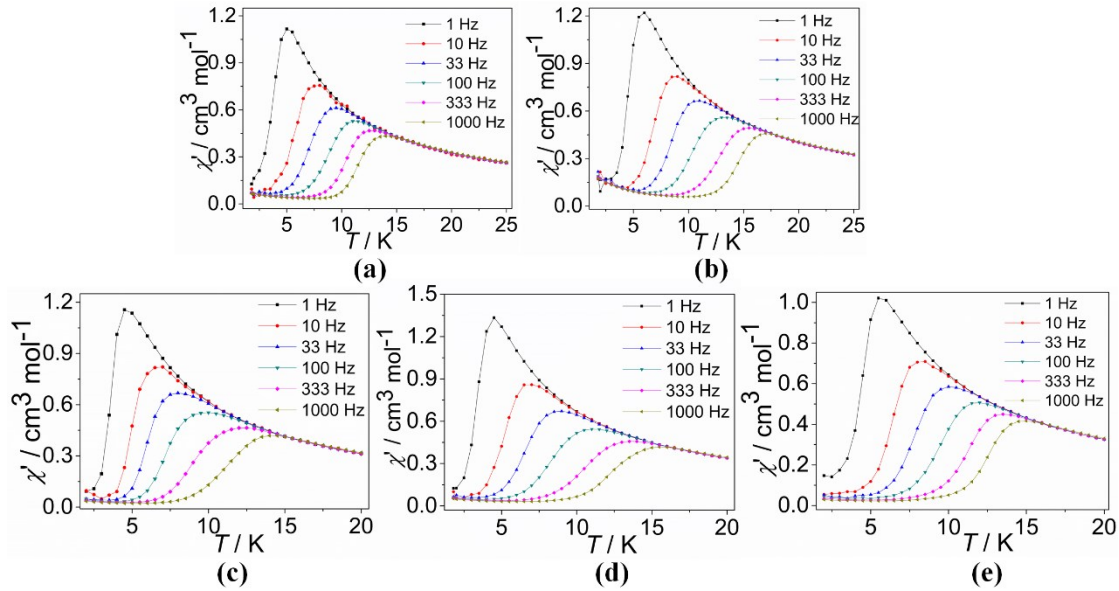


Fig. S13 Temperature dependent in-phase (χ') of the ac susceptibilities for **1** (a), **2** (b), **3**(c), **4** (d) and **5** (e) under the external dc fields.

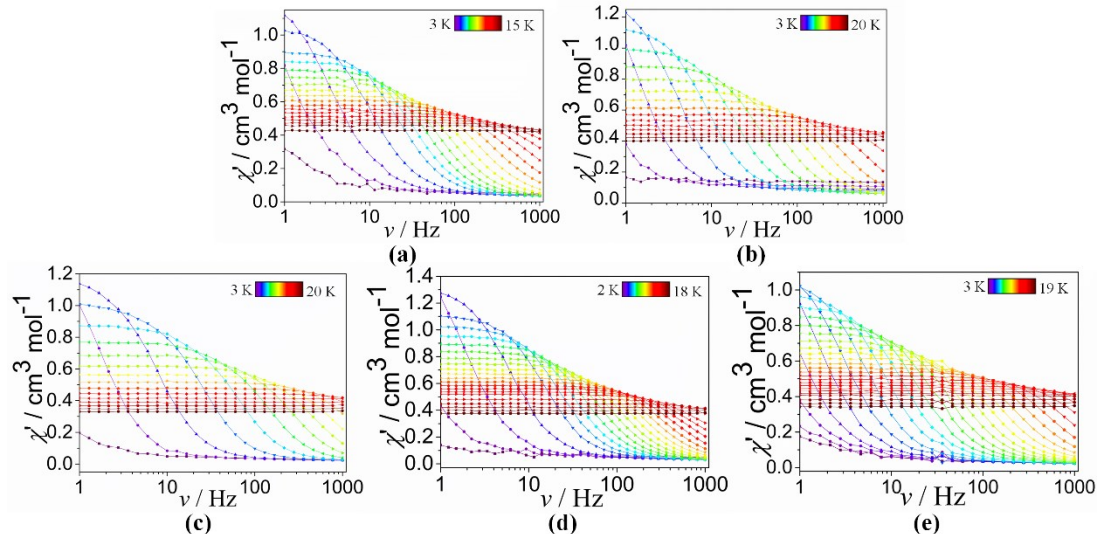


Fig. S14 Frequency dependent in-phase (χ') of the ac susceptibilities for **1** (a), **2** (b), **3**(c), **4** (d) and **5** (e) under the external dc fields.

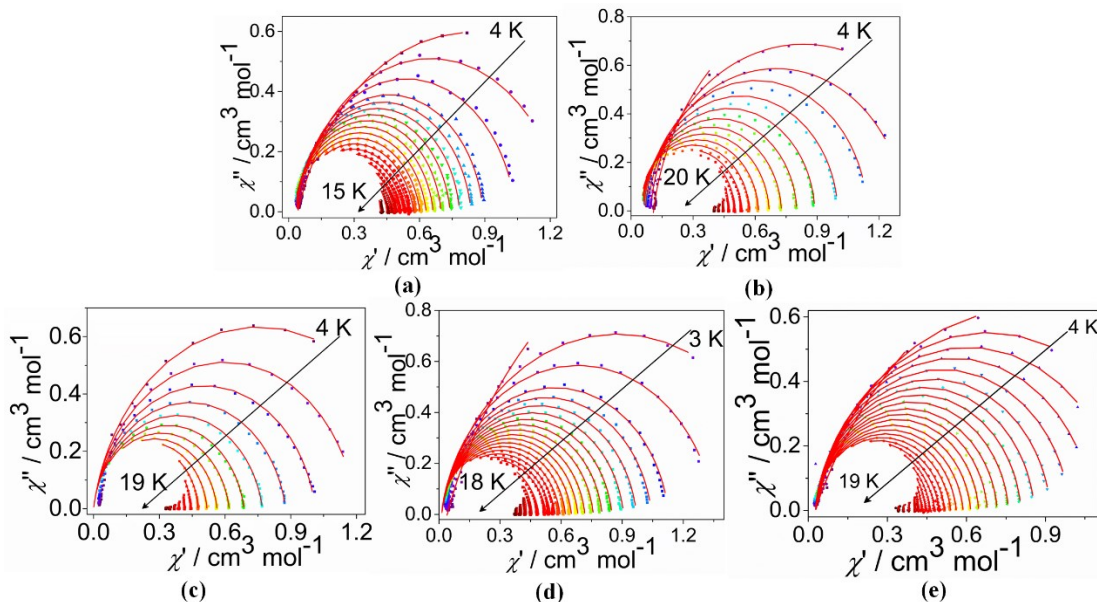


Fig. S15 Cole-Cole plots under the static dc fields for **1** (a), **2** (b), **3** (c), **4** (d) and **5** (e). The solid lines represent the best fit to the measured results.

Table S1. Crystal Data and Structure Refinement Details for 1-5.

	1	2	3	4	5
Empirical formula	C ₅₂ H ₃₁ BrDyF ₉ N ₂ O ₆	C ₅₂ H ₃₀ Br ₂ DyF ₉ N ₂ O ₆	C ₅₄ H ₃₆ DyF ₉ N ₂ O ₆	C ₆₀ H ₄₈ DyF ₉ N ₂ O ₆	C ₅₄ H ₃₆ DyF ₉ N ₂ O ₆
Formula weight	1193.20	1272.10	1142.35	1226.50	1142.35
Crystal system	orthorhombic	monoclinic	orthorhombic	triclinic	monoclinic
Space group	Pca2 ₁	P2 ₁ /n	Pca2 ₁	P ¹	P2 ₁ /n
Temperature (K)	296.0	293.0	150.0	150.0	296.0
<i>a</i> (Å)	20.699(5)	18.614(5)	20.2733(19)	12.6768(13)	11.554(2)
<i>b</i> (Å)	11.435(3)	11.155(3)	11.7442(10)	15.0227(14)	28.108(5)
<i>c</i> (Å)	20.275(5)	23.874(6)	19.7019(18)	16.5274(14)	15.250(3)
α (°)	90	90	90	81.837(7)	90
β (°)	90	101.322(8)	90	73.573(8)	104.622(5)
γ (°)	90	90	90	66.289(9)	90
<i>V</i> (Å ³)	4799.0(19)	4861(2)	4690.9(7)	2762.7(5)	4792.3(15)
<i>Z</i>	4	4	4	2	4
μ (mm ⁻¹)	2.477	3.268	1.683	1.632	1.648
Unique reflections	10550	8469	12358	9615	11028
Observed reflections	43228	77215	47951	15207	41674
<i>R</i> _{int}	0.0421	0.1069	0.0254	0.0556	0.1103
Final R indices [I > 2σ(I)]	R ₁ = 0.0322 wR ₂ = 0.0709	R ₁ = 0.0513 wR ₂ = 0.0823	R ₁ = 0.0200 wR ₂ = 0.0435	R ₁ = 0.0525 wR ₂ = 0.1266	R ₁ = 0.0851 wR ₂ = 0.2003
R indices (all data)	R ₁ = 0.0502 wR ₂ = 0.0780	R ₁ = 0.1210 wR ₂ = 0.0985	R ₁ = 0.0238 wR ₂ = 0.0452	R ₁ = 0.0729 wR ₂ = 0.1410	R ₁ = 0.1732 wR ₂ = 0.2487

Table S2. Selected bond lengths (Å) and bond angles (°) for **1-5**.

Complex 1			
Dy(1)-O(5)	2.328(5)	O(3)-Dy(1)-O(6)	143.84(15)
Dy(1)-O(2)	2.305(4)	O(3)-Dy(1)-N(1)	73.44(16)
Dy(1)-O(4)	2.298(4)	O(4)-Dy(1)-O(1)	118.18(16)
Dy(1)-O(6)	2.341(4)	O(4)-Dy(1)-O(2)	74.02(15)
Dy(1)-O(3)	2.337(4)	O(4)-Dy(1)-O(3)	71.92(15)

Dy(1)-O(1)	2.331(5)	O(4)-Dy(1)-O(5)	77.52(15)
Dy(1)-N(2)	2.555(6)	O(4)-Dy(1)-O(6)	144.03(15)
Dy(1)-N(1)	2.534(6)	O(4)-Dy(1)-N(1)	135.37(17)
O(1)-Dy(1)- O(3)	79.82(18)	O(4)-Dy(1)-N(2)	81.15(17)
O(1)-Dy(1)- O(6)	76.98(16)	O(5)-Dy(1)-O(1)	140.17(17)
O(1)-Dy(1)- N(1)	81.7(2)	O(5)-Dy(1)-O(3)	138.81(16)
O(1)-Dy(1)- N(2)	141.7(2)	O(5)-Dy(1)-O(6)	72.19(15)
O(2)-Dy(1)- O(1)	73.43(16)	O(5)-Dy(1)-N(2)	73.05(15)
O(2)-Dy(1)- O(3)	118.48(16)	O(5)-Dy(1)-N(1)	113.73(18)
O(2)-Dy(1)- O(5)	77.17(15)	O(6)-Dy(1)-N(1)	76.06(16)
O(2)-Dy(1)- O(6)	80.66(14)	O(6)-Dy(1)-N(2)	107.40(16)
O(2)-Dy(1)- N(1)	149.12(19)	O(3)-Dy(1)-N(2)	75.49(18)
O(2)-Dy(1)- N(2)	144.59(18)	N(2)-Dy(1)-N(1)	63.5(2)

Complex 2			
Dy(1)-O(1)	2.327(4)	O(4)-Dy(1)- O(1)	125.35(14)
Dy(1)-O(2)	2.319(4)	O(4)-Dy(1)- O(2)	75.23(14)
Dy(1)-O(3)	2.319(4)	O(4)-Dy(1)- O(3)	72.19(15)
Dy(1)-O(4)	2.294(4)	O(4)-Dy(1)- O(5)	142.75(14)
Dy(1)-O(5)	2.353(4)	O(4)-Dy(1)- O(6)	74.02(14)
Dy(1)-O(6)	2.341(4)	O(4)-Dy(1)- N(1)	134.87(15)
Dy(1)-N(1)	2.543(4)	O(4)-Dy(1)- N(2)	78.78(14)
Dy(1)-N(2)	2.552(4)	O(5)-Dy(1)- N(1)	73.70(14)
O(1)-Dy(1)- O(5)	75.75(14)	O(5)-Dy(1)-N(2)	104.58(14)
O(1)-Dy(1)- O(6)	137.90(14)	O(6)-Dy(1)- O(5)	71.37(14)
O(1)-Dy(1)- N(1)	79.69(14)	O(6)-Dy(1)- N(1)	114.33(14)
O(1)-Dy(1)- N(2)	140.07(14)	O(6)-Dy(1)- N(2)	74.73(14)
O(2)-Dy(1)- O(1)	72.35(13)	N(1)-Dy(1)- N(2)	62.91(14)
O(2)-Dy(1)- O(3)	110.65(14)	C(2)-O(1)- Dy(1)	132.0(4)
O(2)-Dy(1)- O(5)	85.15(14)	C(4)-O(2)- Dy(1)	137.6(4)
O(2)-Dy(1)- O(6)	79.28(14)	C(16)-O(3)- Dy(1)	133.9(4)
O(2)-Dy(1)- N(1)	148.36(15)	C(18)-O(4)- Dy(1)	140.8(4)
O(2)-Dy(1)- N(2)	147.31(14)	C(30)-O(5)- Dy(1)	126.4(4)
O(3)-Dy(1)- O(1)	79.71(15)	C(32)-O(6)- Dy(1)	126.7(4)
O(3)-Dy(1)- O(5)	145.04(15)	C(43)-N(1)- Dy(1)	119.7(4)
O(3)-Dy(1)- O(6)	140.51(14)	C(47)-N(1)- Dy(1)	121.7(3)
O(3)-Dy(1)- N(1)	77.74(15)	C(48)-N(2)- Dy(1)	122.1(4)
O(3)-Dy(1)- N(2)	79.19(14)	C(52)-N(2)- Dy(1)	120.3(3)

Complex 3			
Dy(1)-O(3)	2.324(2)	O(4)-Dy(1)-N(1)	137.92(8)
Dy(1)-O(6)	2.338(2)	O(4)-Dy(1)-N(2)	77.85(8)
Dy(1)-O(1)	2.305(2)	O(4)-Dy(1)-O(2)	81.15(7)
Dy(1)-O(5)	2.319(2)	O(4)-Dy(1)-O(6)	141.64(7)

Dy(1)-O(4)	2.331(2)	O(5)-Dy(1)-N(1)	106.74(8)
Dy(1)-O(2)	2.343(2)	O(5)-Dy(1)-N(2)	75.52(8)
Dy(1)-N(1)	2.535(2)	O(5)-Dy(1)-O(2)	147.87(7)
Dy(1)-N(2)	2.530(3)	O(5)-Dy(1)-O(3)	79.69(7)
N(1)-Dy(1)-N(2)	64.10(9)	O(5)-Dy(1)-O(4)	78.73(7)
O(1)-Dy(1)-N(1)	71.46(7)	O(5)-Dy(1)-O(6)	71.96(7)
O(1)-Dy(1)-N(2)	139.15(8)	O(6)-Dy(1)-N(1)	75.55(8)
O(1)-Dy(1)-O(2)	73.41(13)	O(6)-Dy(1)-N(2)	116.67(8)
O(1)-Dy(1)-O(3)	74.36(7)	O(6)-Dy(1)-O(2)	135.41(7)
O(1)-Dy(1)-O(4)	119.58(7)	C(2)-O(1)-Dy(1)	130.8(3)
O(1)-Dy(1)-O(5)	140.60(7)	C(43)-N(1)-Dy(1)	120.5(2)
O(1)-Dy(1)-O(6)	74.04(7)	C(47)-N(1)-Dy(1)	117.9(2)
O(2)-Dy(1)-N(1)	73.07(8)	C(48)-N(2)-Dy(1)	120.4(2)
O(2)-Dy(1)-N(2)	75.94(8)	C(52)-N(2)-Dy(1)	121.0(2)
O(3)-Dy(1)-N(1)	149.14(8)	C(11)-O(1)-Dy(1)	140.60(18)
O(3)-Dy(1)-N(2)	144.50(8)	C(13)-O(2)-Dy(1)	131.91(19)
O(3)-Dy(1)-O(2)	117.52(7)	C(25)-O(3)-Dy(1)	138.6(2)
O(3)-Dy(1)-O(4)	72.66(7)	C(27)-O(4)-Dy(1)	131.16(19)
O(3)-Dy(1)-O(6)	78.13(7)	C(36)-O(5)-Dy(1)	133.65(19)

Complex 4			
Dy(1)-O(1)	2.317(3)	O(4)-Dy(1)-O(6)	76.70(13)
Dy(1)-O(2)	2.321(4)	O(4)-Dy(1)-N(1)	81.77(14)
Dy(1)-O(3)	2.335(4)	O(4)-Dy(1)-N(2)	133.89(14)
Dy(1)-O(4)	2.291(4)	O(5)-Dy(1)-O(1)	140.50(13)
Dy(1)-O(5)	2.316(3)	O(5)-Dy(1)-O(2)	78.69(13)
Dy(1)-O(6)	2.331(3)	O(5)-Dy(1)-O(3)	76.07(14)
Dy(1)-N(1)	2.528(4)	O(5)-Dy(1)-O(6)	72.03(12)
Dy(1)-N(2)	2.523(4)	O(5)-Dy(1)-N(1)	141.25(13)
O(1)-Dy(1)-O(2)	72.90(12)	O(5)-Dy(1)-N(2)	80.60(13)
O(1)-Dy(1)-O(3)	140.90(13)	O(6)-Dy(1)-O(3)	115.54(14)
O(1)-Dy(1)-O(6)	76.87(12)	O(6)-Dy(1)-N(1)	146.67(13)
O(1)-Dy(1)-N(1)	73.41(13)	O(6)-Dy(1)-N(2)	147.13(13)
O(1)-Dy(1)-N(2)	117.18(14)	N(2)-Dy(1)-N(1)	63.26(13)
O(2)-Dy(1)-O(3)	142.92(13)	C(2)-O(1)-Dy(1)	130.8(3)
O(2)-Dy(1)-O(6)	81.09(13)	C(4)-O(2)-Dy(1)	135.7(3)
O(2)-Dy(1)-N(1)	103.90(14)	C(16)-O(3)-Dy(1)	134.2(3)
O(2)-Dy(1)-N(2)	75.90(14)	C(18)-O(4)-Dy(1)	139.8(3)
O(3)-Dy(1)-N(1)	80.47(15)	C(30)-O(5)-Dy(1)	132.8(3)
O(3)-Dy(1)-N(2)	73.55(15)	C(32)-O(6)-Dy(1)	138.4(3)
O(4)-Dy(1)-O(1)	76.10(13)	C(43)-N(1)-Dy(1)	119.7(3)
O(4)-Dy(1)-O(2)	145.15(12)	C(47)-N(1)-Dy(1)	123.1(3)
O(4)-Dy(1)-O(3)	71.72(13)	C(48)-N(1)-Dy(1)	122.8(3)
O(4)-Dy(1)-O(5)	118.35(14)	C(52)-N(1)-Dy(1)	120.0(3)

Complex 5			
Dy(1)-O(1)	2.351(7)	O(5)-Dy(1)-O(2)	151.5(2)
Dy(1)-O(2)	2.344(7)	O(5)-Dy(1)-O(3)	133.7(3)
Dy(1)-O(3)	2.352(7)	O(5)-Dy(1)-O(4)	75.8(3)
Dy(1)-O(4)	2.335(7)	O(5)-Dy(1)-N(1)	74.5(3)
Dy(1)-O(5)	2.332(8)	O(5)-Dy(1)-N(2)	117.8(3)
Dy(1)-O(6)	2.319(7)	O(6)-Dy(1)-O(1)	154.6(3)
Dy(1)-N(1)	2.538(8)	O(6)-Dy(1)-O(2)	133.6(3)
Dy(1)-N(2)	2.518(8)	O(6)-Dy(1)-O(3)	73.9(3)
O(1)-Dy(1)-O(3)	121.5(3)	O(6)-Dy(1)-O(4)	87.2(3)
O(1)-Dy(1)-N(1)	75.8(3)	O(6)-Dy(1)-O(5)	72.4(3)
O(1)-Dy(1)-N(2)	124.1(3)	O(6)-Dy(1)-N(1)	103.4(3)
O(1)-Dy(1)-O(2)	71.8(3)	O(6)-Dy(1)-N(2)	75.2(3)
O(2)-Dy(1)-O(3)	73.1(2)	N(2)-Dy(1)-N(1)	63.5(3)
O(2)-Dy(1)-N(1)	86.0(3)	C(2)-O(1)-Dy(1)	131.8(7)
O(2)-Dy(1)-N(2)	68.9(3)	C(4)-O(2)-Dy(1)	139.0(7)
O(3)-Dy(1)-N(1)	144.8(3)	C(16)-O(3)-Dy(1)	128.9(6)
O(3)-Dy(1)-N(2)	82.4(3)	C(18)-O(4)-Dy(1)	133.8(7)
O(4)-Dy(1)-O(1)	80.1(3)	C(30)-O(5)-Dy(1)	132.0(7)
O(4)-Dy(1)-O(2)	111.9(3)	C(32)-O(6)-Dy(1)	138.5(7)
O(4)-Dy(1)-O(3)	71.6(3)	C(43)-N(1)-Dy(1)	119.8(7)
O(4)-Dy(1)-N(1)	143.5(3)	C(47)-N(1)-Dy(1)	120.5(6)
O(4)-Dy(1)-N(2)	151.8(3)	C(48)-N(2)-Dy(1)	120.5(6)
O(5)-Dy(1)-O(1)	83.1(3)	C(52)-N(2)-Dy(1)	121.2(7)

Table S3. Dy (III) ions geometry analysis of **1-5** by SHAPE 2.1 software.

Configuration	ABOXIY, 1	ABOXIY, 2	ABOXIY, 3	ABOXIY, 4	ABOXIY, 5
Hexagonal bipyramid (D_{6h})	16.942	16.505	15.512	15.992	12.969
Cube (O_h)	9.979	10.182	9.566	9.912	6.552
Square antiprism (D_{4d})	0.451	0.753	0.525	0.624	1.348
Triangular dodecahedron (D_{2d})	2.363	1.516	2.257	1.831	1.056
Johnson gyrobifastigium J26 (D_{2d})	16.263	15.306	14.984	15.613	15.261
Johnson elongated triangular bipyramid J14 (D_{3h})	27.488	28.213	27.668	27.796	28.575
Biaugmented trigonal prism J50 (C_{2v})	2.737	2.752	2.473	2.382	3.084
Biaugmented trigonal prism (C_{2v})	2.152	2.059	1.960	1.817	2.455
Snub sphenoid J84 (D_{2d})	5.296	4.273	5.013	4.740	4.497
Triakis tetrahedron (T_d)	10.732	10.968	10.417	10.714	7.336

Elongated trigonal bipyramidal (D_{3h})	23.559	23.780	23.624	23.772	23.409
---	--------	--------	--------	--------	--------

Table S4. Relevant structural parameters in square anti-prism geometry, α angle and ϕ angle for **1-4**.

α angle (°)	1	ϕ angle (°)	1
O1	60.799	O5-Dy-O4	45.679
O2	58.376	O4-Dy-N2	48.407
N1	53.598	O2-Dy-O5	42.573
N2	48.803	O2-Dy-O6	43.302
O3	60.129	O3-Dy-N1	40.889
O4	57.404	O3-Dy-N2	43.46
O5	60.164	O6-Dy-O1	48.562
O6	58.593	O1-Dy-N1	47.364
Deviation	57.233	Deviation	45.030
Sum of deviation to ideal 54.74°	2.493	Sum of deviation to ideal 45°	0.030

α angle (°)	2	ϕ angle (°)	2
O1	63.564	O1-Dy-O5	48.851
O2	54.073	O1-Dy-N1	46.184
N1	53.028	O2-Dy-O5	44.477
N2	48.704	O2-Dy-O6	41.207
O3	56.588	O3-Dy-N1	40.711
O4	61.814	O3-Dy-N2	43.284
O5	55.88	O4-Dy-O6	45.686
O6	61.291	O4-Dy-N2	50.037
Deviation	56.868	Deviation	45.055
Sum of deviation to ideal 54.74°	2.128	Sum of deviation to ideal 45°	0.055

α angle (°)	3	ϕ angle (°)	3
O1	57.851	O1-Dy-O6	45.777
O2	60.185	O1-Dy-N1	44.008
N1	49.381	O2-Dy-N1	41.841
N2	54.550	O2-Dy-N2	48.388

O3	57.395	O3-Dy-O5	44.669
O4	61.754	O3-Dy-O6	45.558
O5	57.369	O4-Dy-O5	42.084
O6	62.123	O4-Dy-N2	47.701
Deviation	57.576	Deviation	45.003
Sum of deviation to ideal	2.836	Sum of deviation to ideal	0.003
54.74°		45°	

α angle (°)	4	ϕ angle (°)	4
O1	62.264	O1-Dy-O6	41.560
O2	56.939	O1-Dy-O4	44.139
N1	46.945	O2-Dy-O5	49.813
N2	54.959	O2-Dy-O6	44.906
O3	57.458	O3-Dy-N1	44.552
O4	59.516	O3-Dy-N2	39.641
O5	58.822	O4-Dy-O1	44.139
O6	58.082	O4-Dy-N1	50.182
Deviation	56.873	Deviation	44.867
Sum of deviation to ideal	2.133	Sum of deviation to ideal	0.133
54.74°		45°	

Table S5. Crystal field parameters for **1-5** fitted from $\chi_M T$ vs. T and M vs. H simultaneously.

	B_0^2	B_0^4	B_2^4	B_0^6	g
1	481	-10	179	8	
2	282	-76	27	-426	$g_x = g_y = 1.13, g_z = 1.62$
3	25	127	1280	338	
4	-221	85	995	19	
5	-360	72	1011	-19	

Table S6. Energy levels and g for **1-5** fitted from $\chi_M T$ vs. T and M vs. H simultaneously.

KDs	1		2		3	
	E/cm^{-1}	g	E/cm^{-1}	g	E/cm^{-1}	g
1	0	0.0000 0.0000 19.9230	0	0.0000 0.0000 24.2959	0	0.0004 0.0066 17.1223

2	94	0.0000 0.0000 17.2586	141	0.0000 0.0000 11.3440	57	0.6460 2.4864 17.4283
3	213	0.0000 0.0000 14.6903	161	0.0000 0.0000 14.5800	366	0.0764 0.0785 15.4029
4	317	0.0000 0.0001 12.0612	176	0.0004 0.0004 8.1001	458	3.2004 6.4134 8.1014
5	396	0.0847 0.1121 9.3601	219	0.0000 0.0000 17.8201	794	1.4295 1.4902 6.7636
6	443	3.6826 5.4555 5.7376	262	0.1642 0.1642 4.8595	824	0.0885 0.1291 18.6467
7	470	1.7573 5.1389 11.6793	404	0.0000 0.0000 21.0599	996	0.0707 0.1245 11.9002
8	513	0.0066 0.0398 18.7480	429	1.6195 8.8754 9.2039	1079	0.0607 0.1145 9.8486
KDs		4		5		
		E/cm^{-1}	g	E/cm^{-1}	g	
1	0	0.0351 0.0448 19.2174		0.1046 0.1879 19.3334		
2	170	6.1174 7.2742 8.0199	153	0.2972 2.5281 12.7694		
3	189	0.9674 1.8274 14.1202	189	2.7519 7.3756 11.9988		
4	222	4.0808 4.6249 8.6008	248	1.3585 5.5176 9.8502		
5	296	1.7911 7.4430 8.6394	296	2.6661 3.4102 13.3867		
6	329	2.3871 4.7180 11.7344	349	0.7005 1.0388 15.2153		
7	508	0.0048 0.0691 14.6372	589	0.0006 0.0265 15.9493		

8	536	0.0248 0.0635 16.0517	603	0.0069 0.0270 16.9433
---	-----	-----------------------------	-----	-----------------------------

Table S7. Relaxation fitting parameters from least-squares fitting of $\chi(f)$ data under zero dc field of **1**.

T(K)	χ_T	χ_S	α
3.0	2.146	0.238	0.159
4.0	1.610	0.182	0.154
5.0	1.288	0.149	0.145
6.0	1.072	0.128	0.130
6.5	0.989	0.120	0.120
7.0	0.918	0.112	0.110
7.5	0.856	0.105	0.100
8.0	0.802	0.098	0.090
8.5	0.755	0.091	0.081
9.0	0.713	0.084	0.072
9.5	0.675	0.079	0.065
10.0	0.641	0.073	0.060
10.5	0.611	0.070	0.055
11.0	0.583	0.069	0.052
12.0	0.534	0.066	0.052
13.0	0.494	0.022	0.056
14.0	0.459	0.010	0.032

Table S8. Relaxation fitting parameters from least-squares fitting of $\chi(f)$ data under zero dc field of **2**.

T(K)	χ_T	χ_S	α
3.0	2.738	0.306	0.168
4.0	2.042	0.231	0.168
5.0	1.628	0.185	0.166
6.0	1.352	0.158	0.155
6.5	1.247	0.147	0.147
7.0	1.155	0.138	0.137
7.5	1.077	0.129	0.126
8.0	1.007	0.122	0.114
8.5	0.947	0.115	0.102
9.0	0.893	0.107	0.091
9.5	0.845	0.101	0.081
10.0	0.802	0.094	0.072
10.5	0.763	0.087	0.063
11.0	0.728	0.081	0.056
11.5	0.696	0.074	0.050
12.0	0.666	0.068	0.045
12.5	0.639	0.063	0.041
13.0	0.615	0.057	0.038

13.5	0.592	0.051	0.035
14.0	0.570	0.046	0.031
15.0	0.533	0.025	0.029
16.0	0.500	0.014	0.015
17.0	0.472	0.003	0.013

Table S9. Relaxation fitting parameters from least-squares fitting of $\chi(f)$ data under zero dc field of **3**.

T(K)	χ_T	χ_S	α
3.0	2.060	0.306	0.152
4.0	1.549	0.225	0.154
5.0	1.242	0.179	0.152
6.0	1.036	0.152	0.140
7.0	0.889	0.133	0.125
8.0	0.778	0.121	0.105
9.0	0.692	0.104	0.092
10.0	0.623	0.091	0.078
11.0	0.567	0.080	0.059
12.0	0.520	0.045	0.045
13.0	0.480	0.019	0.018
14.0	0.447	0.021	0.011
15.0	0.418	0.029	0.015
16.0	0.393	0.048	0.019

Table S10. Relaxation fitting parameters from least-squares fitting of $\chi(f)$ data under zero dc field of **4**.

T(K)	χ_T	χ_S	α
2.0	3.489	0.279	0.207
3.0	2.319	0.192	0.205
4.0	1.732	0.148	0.196
4.5	1.535	0.134	0.187
5.0	1.377	0.124	0.175
5.5	1.249	0.115	0.162
6.0	1.141	0.108	0.147
6.5	1.050	0.100	0.133
7.0	0.973	0.093	0.118
7.5	0.906	0.086	0.106
8.0	0.849	0.079	0.095
8.5	0.797	0.073	0.085
9.0	0.752	0.067	0.076
9.5	0.712	0.061	0.069
10.0	0.675	0.055	0.063
10.5	0.643	0.049	0.059
11.0	0.614	0.043	0.057
11.5	0.587	0.037	0.055
12.0	0.562	0.034	0.054

12.5	0.539	0.033	0.054
13.0	0.519	0.033	0.052

Table S11. Relaxation fitting parameters from least-squares fitting of $\chi(f)$ data under zero dc field of **5**.

T(K)	χ_T	χ_s	α
3.0	2.131	0.187	0.134
3.5	1.828	0.163	0.135
4.0	1.602	0.142	0.136
4.5	1.425	0.128	0.136
5.0	1.283	0.116	0.136
5.5	1.167	0.108	0.135
6.0	1.070	0.101	0.132
6.5	0.988	0.096	0.127
7.0	0.918	0.089	0.124
7.5	0.857	0.086	0.116
8.0	0.803	0.084	0.108
8.5	0.756	0.082	0.099
9.0	0.714	0.080	0.089
9.5	0.676	0.079	0.079
10.0	0.642	0.075	0.068
10.5	0.612	0.067	0.058
11.0	0.584	0.059	0.047
11.5	0.558	0.049	0.039
12.0	0.535	0.029	0.035
12.5	0.514	0.009	0.032
13.0	0.495	0.002	0.019
13.5	0.476	0.002	0.004
14.0	0.459	0.003	0.004

Table S12. Relaxation fitting parameters from least-squares fitting of $\chi(f)$ data under 1500 Oe dc field of **1**.

T(K)	χ_T	χ_s	α
4.0	1.664	0.042	0.192
5.0	1.284	0.039	0.125
6.0	1.059	0.035	0.092
7.0	0.907	0.031	0.073
7.5	0.849	0.029	0.074
8.0	0.797	0.028	0.070
8.5	0.752	0.026	0.073
9.0	0.709	0.025	0.077
9.5	0.673	0.030	0.089
10.0	0.640	0.024	0.101
10.5	0.611	0.028	0.112
11.0	0.582	0.032	0.125
11.5	0.557	0.040	0.136

12.0	0.536	0.049	0.150
12.5	0.513	0.072	0.141
13.0	0.492	0.079	0.136
13.5	0.475	0.085	0.134
14.0	0.458	0.066	0.118
15.0	0.428	0.058	0.056

Table S13. Relaxation fitting parameters from least-squares fitting of $\chi(f)$ data under 1200 Oe dc field of **2**.

T(K)	χ_T	χ_S	α
4.0	1.801	0.102	0.218
5.0	1.844	0.019	0.173
6.0	1.378	0.018	0.107
7.0	1.141	0.068	0.041
8.0	0.998	0.061	0.037
9.0	0.887	0.055	0.034
10.0	0.799	0.049	0.037
11.0	0.726	0.042	0.038
12.0	0.666	0.037	0.041
13.0	0.615	0.031	0.044
14.0	0.571	0.030	0.045
15.0	0.533	0.033	0.042
16.0	0.500	0.015	0.030
17.0	0.472	0.018	0.037
18.0	0.446	0.015	0.058
19.0	0.423	0.016	0.009
20.0	0.402	0.014	0.014

Table S14. Relaxation fitting parameters from least-squares fitting of $\chi(f)$ data under 1200 Oe dc field of **3**.

T(K)	χ_T	χ_S	α
4.0	1.505	0.002	0.108
5.0	1.198	0.005	0.101
6.0	1.011	0.001	0.105
7.0	0.874	0.002	0.106
8.0	0.769	0.003	0.108
9.0	0.686	0.004	0.106
10.0	0.618	0.006	0.102
11.0	0.563	0.001	0.094
12.0	0.517	0.003	0.077
13.0	0.477	0.004	0.053
14.0	0.444	0.001	0.032
15.0	0.415	0.001	0.040
16.0	0.390	0.003	0.053
17.0	0.368	0.005	0.060
18.0	0.348	0.001	0.053

19.0	0.331	0.001	0.072
------	-------	-------	-------

Table S15. Relaxation fitting parameters from least-squares fitting of $\chi(f)$ data under 1200 Oe dc field of **4**.

T(K)	χ_T	χ_S	α
3.0	0.187	0.012	0.226
4.0	1.743	0.031	0.132
5.0	1.355	0.048	0.093
6.0	1.125	0.095	0.078
6.5	1.040	0.011	0.079
7.0	0.965	0.012	0.078
7.5	0.902	0.016	0.078
8.0	0.844	0.015	0.079
8.5	0.795	0.011	0.078
9.0	0.752	0.073	0.080
9.5	0.710	0.011	0.079
10.0	0.674	0.095	0.081
10.5	0.643	0.010	0.084
11.0	0.614	0.081	0.090
11.5	0.587	0.011	0.097
12.0	0.563	0.018	0.107
12.5	0.540	0.027	0.116
13.0	0.520	0.040	0.121
14.0	0.482	0.085	0.104
15.0	0.449	0.017	0.057
16.0	0.422	0.042	0.035
17.0	0.398	0.069	0.044
18.0	0.376	0.010	0.056

Table S16. Relaxation fitting parameters from least-squares fitting of $\chi(f)$ data under 1200 Oe dc field of **5**.

T(K)	χ_T	χ_S	α
4.0	2.571	0.025	0.245
4.5	1.624	0.028	0.156
5.0	1.332	0.029	0.107
5.5	1.187	0.027	0.088
6.0	1.079	0.029	0.069
6.5	0.993	0.028	0.064
7.0	0.919	0.027	0.059
7.5	0.858	0.028	0.055
8.0	0.807	0.028	0.054
8.5	0.760	0.029	0.053
9.0	0.717	0.029	0.056
9.5	0.679	0.030	0.054
10.0	0.646	0.032	0.055
10.5	0.616	0.028	0.068

11.0	0.587	0.026	0.074
11.5	0.561	0.027	0.075
12.0	0.540	0.020	0.089
12.5	0.517	0.016	0.093
13.0	0.497	0.006	0.098
13.5	0.479	0.002	0.098
14.0	0.462	0.003	0.083
14.5	0.446	0.001	0.064
15.0	0.431	0.001	0.046
15.5	0.419	0.001	0.034
16.0	0.406	0.0001	0.025
17.0	0.382	0.0004	0.024
18.0	0.362	0.0006	0.030
19.0	0.343	0.0007	0.038

Table S17. Calculated energy levels (cm^{-1}), \mathbf{g} (g_x , g_y , g_z) tensors and predominant m_J values of the lowest eight Kramers doublets (KDs) of complexes **1-5** using CASSCF/RASSI-SO with MOLCAS 8.4.

KDs	1			2			3		
	E/cm^{-1}	\mathbf{g}	m_J	E/cm^{-1}	\mathbf{g}	m_J	E/cm^{-1}	\mathbf{g}	m_J
1	0.0	0.004		0.0	0.003		0.0	0.082	
		0.009	$\pm 15/2$		0.007	$\pm 15/2$		0.118	
		19.561			19.499			19.407	
2	121.7	0.218		142.5	0.159		76.1	0.617	
		0.444	$\pm 13/2$		0.208	$\pm 13/2$		0.730	
		16.673			16.174			18.857	
3	162.8	2.802		209.5	2.831		110.6	0.550	
		5.776	$\pm 9/2$		3.167	$\pm 3/2$		1.711	
		12.612			15.452			15.632	
4	186.9	8.072		231.5	1.568		155.5	3.076	
		4.172	$\pm 7/2$		4.360	$\pm 9/2$		5.273	
		0.053			9.748			11.268	
5	226.0	1.775		269.6	3.558		207.8	3.136	
		2.707	$\pm 5/2$		5.151	$\pm 5/2$		4.745	
		11.587			8.185			12.660	
6	275.4	0.646		291.5	1.111		275.0	0.082	
		0.837	$\pm 3/2$		3.098	$\pm 7/2$		1.792	
		16.362			14.836			17.914	
7	341.1	0.191		362.7	0.181		290.5	0.160	
		0.292	$\pm 1/2$		0.281	$\pm 1/2$		1.529	
		19.510			19.194			17.630	
8	477.1	0.011		465.0	0.036		456.9	0.023	
		0.020	$\pm 11/2$		0.083	$\pm 11/2$		0.045	
		19.729			19.563			19.583	
KDs	4			5					

	E/cm^{-1}	\mathbf{g}	m_J	E/cm^{-1}	\mathbf{g}	m_J
1	0.0	0.006		0.0	0.012	
		0.011	$\pm 15/2$		0.019	$\pm 15/2$
		19.471			19.492	
2	130.3	0.394		153.4	0.999	
		1.030	$\pm 13/2$		2.020	$\pm 13/2$
		15.723			13.547	
3	166.4	1.918		174.1	2.687	
		2.896	$\pm 1/2$		4.466	$\pm 1/2$
		15.702			12.053	
4	201.5	0.288		213.1	2.400	
		3.856	$\pm 9/2$		4.281	$\pm 7/2$
		10.614			10.640	
5	231.0	3.401		285.8	0.597	
		5.565	$\pm 7/2$		3.831	$\pm 5/2$
		10.514			12.136	
6	284.9	0.348		315.8	1.043	
		0.589	$\pm 5/2$		3.086	$\pm 9/2$
		16.747			15.366	
7	321.7	0.173		410.1	0.106	
		0.355	$\pm 3/2$		0.315	$\pm 3/2$
		19.085			16.800	
8	467.3	0.007		462.8	0.071	
		0.013	$\pm 11/2$		0.319	$\pm 11/2$
		19.695			18.245	

Table S18. Wave functions with definite projection of the total moment $| m_J \rangle$ for the lowest two KDs of complexes **1–5** using CASSCF/RASSI-SO with MOLCAS 8.4.

	E/cm^{-1}	wave functions
1	0.0	94% $ \pm 15/2\rangle$
	121.7	78% $ \pm 13/2\rangle$ +14% $ \pm 11/2\rangle$
2	0.0	94% $ \pm 15/2\rangle$
	142.5	82% $ \pm 13/2\rangle$ +12% $ \pm 9/2\rangle$
3	0.0	94% $ \pm 15/2\rangle$
	76.1	12% $ \pm 7/2\rangle$ +17% $ \pm 5/2\rangle$ +26% $ \pm 3/2\rangle$ +32% $ \pm 1/2\rangle$
4	0.0	94% $ \pm 15/2\rangle$
	130.3	74% $ \pm 13/2\rangle$ +12% $ \pm 9/2\rangle$
5	0.0	94% $ \pm 15/2\rangle$
	153.4	54% $ \pm 13/2\rangle$ +26% $ \pm 9/2\rangle$